Proton Binding Characteristics of Branched Polyelectrolytes

Michal Borkovec*

Swiss Federal Institute of Technology, ETH-ITO, Grabenstrasse 3, 8952 Schlieren, Switzerland

Ger J. M. Koper

Leiden Institute of Chemistry, Leiden University, Gorlaeus Laboratories, P.O. Box 9502, 2300 RA Leiden, The Netherlands

Received September 4, 1996; Revised Manuscript Received January 15, 1997[⊗]

ABSTRACT: Acid−base properties of branched, weak polyelectrolytes are analyzed theoretically by means of Ising models with short-range interactions. Assuming that the structure of the branched polyelectrolyte can be approximated by the topology of a tree (no closed loops), the Ising model with nearest neighbor pair interactions can be solved with exact recursion relations. We demonstrate that the branching structure has important implications for the protonation behavior of weak polyelectrolytes. For instance, the protonation a dendritic and a comblike polyelectrolyte proceed rather differently. Within this framework, the titration behavior of branched poly(ethylene imine) can be explained quantitatively.

1. Introduction

Poly(ethylene imine) is not only important in various industrial applications, it also provides an excellent example for a typical but poorly understood feature of weak polyelectrolytes: the proton binding characteristics of linear and branched polyelectrolytes differ substantially.[1−6] For instance, linear poly(ethylene imine) is fully protonated below pH 2, while branched poly(ethylene imine) still carries a substantial fraction of deprotonated amine groups at this pH. The reason for this different behavior is certainly related to the different structure of both polyelectrolytes: While linear poly(ethylene imine) with $-CH_2CH_2NH-$ as the repeating unit contains almost only secondary amine groups with a coordination number of 2 (and just two primary amines as terminal groups), branched poly(ethylene imine) contains, in addition to the secondary groups, significant fractions of primary terminal groups and tertiary amine groups on the branch points so that the ionizable groups have coordination numbers one, two, and three. In both cases, the ionizable groups are chemically very similar and are expected to have comparable microscopic affinities for protons. However, in linear and branched polyelectrolytes, the mutual arrangement of the ionizable groups is very different. As we shall argue below, these different arrangements represent the fundamental reason for the distinct ionization properties of linear and branched polyelectrolytes.

The appropriate framework to discuss such phenomena is the Ising model.[6−10] This model can be used to describe ionization of any polyprotic system; thereby one assigns a two-valued state variable to each ionizable site and expresses the (free) energy of a given protonation state in terms of contributions of individual sites (microscopic pK values) and site interaction energies, where repulsive nearest neighbor pair interactions represent the dominant contributions. This energy is used to weigh the individual configurations in the evaluation of the statistical averages from which the thermodynamic quantities of interest follow. From this framework not only does one recover the classical description of successive ionization equilibria,[11] but also one can also successfully explain the typical two-step ionization process of linear weak polyelectrolytes.[6−10] This characteristic ionization pattern is a consequence of the nearest neighbor pair interactions acting between charged sites along the polymer chain; these repulsive interactions stabilize an intermediate protonation state of alternating protonated and deprotonated groups. This stable state leads to an intermediate plateau in the titration curve and, thus, to two apparent protonation steps. The separation of these protonation steps (on the pH axis) is roughly twice as large as the separation of the two protonation steps of the corresponding diprotic molecular analog; the latter separation is related to the difference of the classical macroscopic pK values of the diprotic molecule. In the language of the Ising model, this separation of the protonation steps is related to the nearest neighbor pair interaction energy. In the case of linear polyelectrolytes, where each group has two nearest neighbors, two interaction energies must be overcome. The separation for the linear polyelectrolyte is therefore twice as large as the separation for the diprotic molecule where each ionizable group has only one nearest neighbor. For linear poly(ethylene imine) the splitting is roughly 4 on the pH scale while in the case ethylenediamine (en) the splitting is about 2. This splitting is related to the pair interaction energy of two amines separated by an ethylene chain; we represent this interaction energy in terms of a dimensionless interaction parameter $\epsilon \simeq 2$ which is chosen to correspond directly to the pH scale (see below).

The interactions between the individual sites act mainly along the polymer chain, while the interactions between sites that are situated on different parts of the chain are much weaker. This type of interaction results from a strong Coulomb repulsion within the polymer backbone of low dielectric constant, but it is screened off very effectively by the electrolyte solution. This observation leads us to the following approximation, which is also applicable for the branched case. We shall only consider interactions between two and three neighboring sites that are directly connected by the polymer chain. Interactions between all other sites will be neglected: in particular interactions between sites which are located on different branches of the chain.

From these considerations it follows that the difference in connectivities between linear and branched

[⊗] Abstract published in *Advance ACS Abstracts,* March 15, 1997.

S0024-9297(96)01312-5 CCC: $14.00

Table 1. Experimental Macroscopic pK_n Values for Tris(2-aminoethyl)amine and Calculations Based on the Ising Model

no. of bound protons n	pK_n		
	simple model[a]	realistic model[b]	exptl values[c]
1	10.60	10.24	10.14
2	9.88	9.49	9.68
3	9.52	8.74	8.74
4	4.00	0.69	<3

[a] Microscopic p$\hat{K}$ for all groups and nearest neighbor pair interaction $\epsilon = 2$ only. [b] The microscopic p$\hat{K}$ values of the primary and tertiary amines are 9.64 and 7.50, respectively. The interaction parameters are for nearest neighbor pairs $\epsilon = 1.85$, nearest neighbor triplets $\lambda = 0.42$, and for next nearest neighbor pairs across a tertiary group $\epsilon' = 0.27$. The latter parameter is derived by fitting this data set. [c] Experimental values at an ionic strength of 0.5 M from ref 12.

structures is indeed the most likely reason for their different acid−base behavior. A tertiary amine group has three nearest neighbors, and if these neighboring groups are protonated, this group can only be protonated if three pair interactions are overcome. This conjecture readily explains why the full protonation of tris(2-aminoethyl)amine (tren) is so difficult (see Table 1). In this molecule, all three primary amine groups protonate around pH 10. The protonation of the central tertiary amine group must be accomplished when all three neighboring amine groups are protonated, which requires the compensation of three pair interactions with $\epsilon \simeq 2$. From the Ising model one thus estimates the last pK to be around 4, which is in the same range as the experimental value.[12] From this perspective, it is clear that the protonation of branched poly(ethylene imine) must be more difficult than that of the linear analog. For the branched polyelectrolyte, we expect the stabilization of an intermediate state, where all primary and secondary groups are protonated but the tertiary groups will remain deprotonated. The protonation of these tertiary groups is more difficult since three pair interactions must be overcome—an essential difference to the linear case where at most two pair interactions become operational.

This qualitative picture was already anticipated 2 decades ago.[3] However, a quantitative analysis of this problem is presently lacking. To tackle this problem on the basis of the Ising models represents the major aim of this paper. We show how to analyze ionization properties of branched weak polyelectrolytes within this framework quantitatively. As an approximation, we assume that closed loops can be neglected in branched polyelectrolytes and model their topology by trees. Ising models on trees can be solved by means of exact recursion relations.[13−15] Such results provide general insight into the ionization behavior of various types of branched polyelectrolytes with dendritic,[16,17] comblike, or randomly branched structures.[1−5] In this paper we shall quantitatively explain the titration curve of branched poly(ethylene imine); the protonation of poly(propylene imine) denrimers can be rationalized using the same model as will be discussed elsewhere.[18]

2. Fundamentals

Ising Model of Proton Binding. In this section we shall briefly summarize how the ionization properties of polyprotic acids and bases can be approached with an Ising model.[6−10] This model introduces a set of state variables $s_1, s_2, ..., s_N$ where $s_i = 0$ if site i is deprotonated and $s_i = 1$ if this site is protonated and N is the total number of ionizable sites.

Free Energy. The free energy of a given protonation state of the molecule is expanded in terms of many-body contributions

$$F(s_1, ..., s_N) = -\sum_i \mu_i s_i + \frac{1}{2!}\sum_{i,j} E_{ij} s_i s_j + \frac{1}{3!}\sum_{i,j,k} L_{ijk} s_i s_j s_k + ... \quad (1)$$

where μ_i are chemical potentials while E_{ij} and L_{ijk} are the pair and triplet interaction energies, respectively. The chemical potential terms are related to the pH value of the solution by

$$\beta\mu_i/\ln 10 = \mathrm{p}\hat{K}_i - \mathrm{pH} \quad (2)$$

where $1/\beta = kT$ is the thermal energy and p$\hat{K}_i$ are the microscopic pK values of site i given that all other groups are deprotonated. The elements of the symmetrical pair interaction E_{ij} matrix will be assumed to be equal to E for the nearest neighbor interactions and to vanish elsewhere. As appropriate for proton binding we consider repulsive (antiferromagnetic) interactions only ($E > 0$). To characterize the strength of the interactions we shall also employ the abbreviations

$$\epsilon_{ij} = \beta E_{ij}/\ln 10 \quad (3)$$

for the pair interactions and

$$\lambda_{ijk} = \beta L_{ijk}/\ln 10 \quad (4)$$

for triplet interactions. The latter parameter, as well as higher order interaction parameters, will be usually set to zero in the present context.

Titration Curve. Thermal expectation values can be evaluated from the grand partition function

$$\Xi = \sum_{s_1,...,s_N} \mathrm{e}^{-\beta F(s_1,...,s_N)} \quad (5)$$

which contains all information of interest. The classical description of polyprotic acids and bases is recovered by considering the fugacity expansion[10]

$$\Xi = \sum_{n=0} K_n z^n \quad (6)$$

where $K_0 = 1$ and z is the activity of the protons in mol/L (pH $= -\log_{10} z$). Realizing that the coefficients K_n entering eq 6 are just the formation constants of the protonation step n, the familiar macroscopic pK values of successive protonation steps of a polyprotic base follow from p$K_n = \log(K_n/K_{n-1})$ for $n = 1, ..., N$. The acid−base titration curve, which is given by the average degree of protonation θ, is given by

$$\theta = \frac{z}{N}\frac{\partial \ln \Xi}{\partial z} \quad (7)$$

If eq 6 is inserted into eq 7, the familiar expression for the titration curve of a polyprotic acid or base is recovered.[10]

Ising Model on Trees. While the grand partition function can be evaluated for infinite linear chains exactly[6−8] analytical results for other infinite lattices are scarce.[13] The alternative to obtain approximate results with Monte Carlo techniques[21] is, even with the powerful computers available today, rather time consuming. However, if we focus on nearest neighbor pair

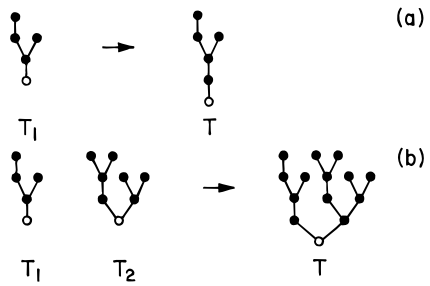

Figure 1. Illustration of the recursion relations of the Ising trees. (a) Attaching one site to an arbitrary tree T_1 leads to a new tree T with its root at the newly attached site (cf. eq 10). (b) Joining two trees T_1 and T_2 together leads to a new tree T with its root at the newly attached site (cf. eq 13).

interactions and treelike structures, we shall demonstrate that one can obtain numerically exact results for rather large systems ($N \simeq 10^4-10^7$). As we shall now demonstrate, these tasks can be achieved by using simple recursion relations. The reader may consider skipping the following mathematical developments and proceed directly to Section 3. We also refer to the Appendix for a summary of graph theoretical terminology which will be used in the remaining part of this section.

Linear Chain. Let us recall the action of the transfer matrix for a linear chain in a slightly more general fashion than discussed in textbooks.[13,21] First, we define the *restricted* partition function of a rooted tree T. This is the partition function of the tree with a fixed (restricted) value of the state variable s_r at the root of the tree, which is labeled by an index r (see Figure 1). The restricted partition function has two values and can be written as

$$\tilde{\Xi}(s) = \sum_{s_1,\ldots,s_N} \mathrm{e}^{-\beta F(s_1,\ldots,s_N)}\, \delta_{s,s_r} \tag{8}$$

where $s = 0,1$ and $\delta_{ss'}$ is unity for $s = s'$ and zero for $s \neq s'$. Note that if $\tilde{\Xi}(s)$ is given, one also knows the partition function Ξ of the entire tree, since

$$\Xi = \sum_s \tilde{\Xi}(s) \tag{9}$$

Suppose for the moment that the restricted partition function $\tilde{\Xi}_1(s)$ of the rooted tree T_1 is known. We now add a new site to the root of the tree T_1 and obtain a new rooted tree T whereby the newly added site is taken to be the root of the new tree (see Figure 1). The restricted partition function $\tilde{\Xi}(s)$ of this new tree T can now be obtained by a linear transformation of the restricted partition function $\tilde{\Xi}_1(s)$ of the old tree T_1. The appropriate recursion relation reads[13,21]

$$\tilde{\Xi}(s) = t^s \sum_{s'} u^{ss'} \tilde{\Xi}_1(s') \tag{10}$$

where $t = e^{\beta\mu}$ is the fugacity of the newly added site and $u = e^{-\beta E}$ parametrizes the nearest neighbor interaction energy E of the newly added bond. Equation 10 is commonly interpreted as a transformation by a 2×2 transfer matrix, whose elements are given by $t^s u^{ss'}$. One possible way to solve the linear chain Ising model is to find the larger eigenvalue of this transfer matrix[13,21]

$$\eta = (1 + tu)/2 + [t + (1 - tu)^2/4]^{1/2} \tag{11}$$

which can be shown to determine the partition function of an infinitely long chain ($N \to \infty$). In this limit the partition function is given by $\Xi \sim \eta^N$. Inserting this relation into eq 7, we obtain the titration curve of a linear polyelectrolyte with nearest neighbor pair interactions[7,8]

$$\theta = [2 + (\eta/t)(1 - tu)/(1 - u + \eta u)]^{-1} \tag{12}$$

General Trees. We are now in position to construct the general recursion relations to evaluate the partition function of arbitrary trees. Suppose that restricted partitions functions $\tilde{\Xi}_1(s)$ and $\tilde{\Xi}_2(s)$ are known for two arbitrary rooted trees T_1 and T_2. If we connect each root of these two trees T_1 and T_2 to a new site, we obtain a new rooted tree T whereby the new site is taken to be the root of the new tree (see Figure 1). The restricted partition function of this new tree $\tilde{\Xi}(s)$ follows from the recursion relation

$$\tilde{\Xi}(s) = t^s \sum_{s',s''} u^{ss'} u^{ss''} \tilde{\Xi}_1(s') \tilde{\Xi}_2(s'') \tag{13}$$

where all variables were already defined in eq 10. We can now generalize eqs 10 and 13, and present a relation for joining l rooted trees together, each described by a restricted partition function $\tilde{\Xi}_k(s)$ ($k = 1, \ldots, l$). The restricted partition function of the resulting tree is given by

$$\tilde{\Xi}(s) = t^s \sum_{s^{(1)},\ldots,s^{(l)}} \prod_{k=1}^{l} u^{ss^{(k)}} \tilde{\Xi}_k(s^{(k)}) \tag{14}$$

Recursive application of eq 14 leads to exact partition functions for arbitrary trees. While the recursion result can be evaluated analytically in special situations only, exact results for arbitrary (and very large) trees can be obtained numerically.

Numerical Implementation. To carry out such calculations we introduce the variable $a = \tilde{\Xi}(1)/\tilde{\Xi}(0)$ which obeys the recursion relation (cf. eq 14)

$$a = t \prod_k \left(\frac{1 + u a_k}{1 + a_k} \right) \tag{15}$$

As above, we employ the notation that subscripted quantities refer to rooted trees prior to the iteration while quantities without a subscript refer to quantities after iteration. From eq 9 the partition function follows:

$$\Xi = (1 + a) \prod_k \Xi_k \tag{16}$$

The recursion relation, which determines the average degree of protonation, can be obtained by applying eq 7 to eq 16. Let us introduce the average number of bound protons $\nu = N\theta$ for which the following recursion relation applies

$$\nu = \frac{b_k a_k}{1 + a_k} + \sum_k \nu_k \tag{17}$$

where $b = (t/a)(\partial a/\partial t)$ obeys

$$b = 1 + \sum_k \frac{(u - 1) a_k b_k}{(1 + u a_k)(1 + a_k)} \tag{18}$$

The recursion procedure is initiated simultaneously for

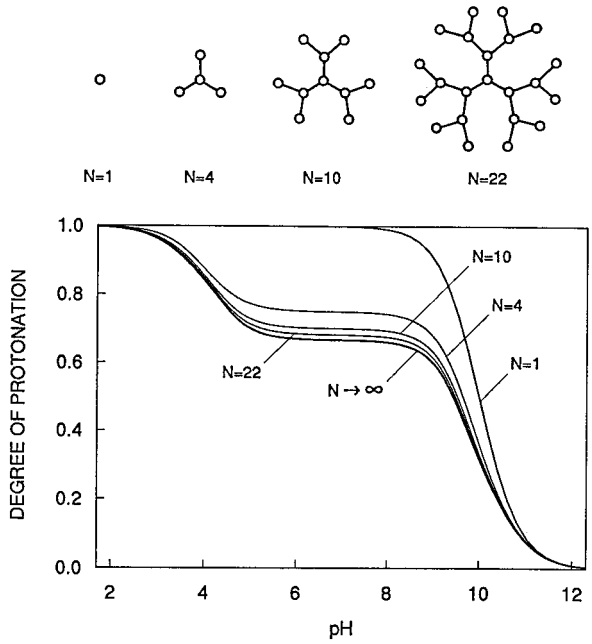

Figure 2. Calculated titration curves for dendrimers with increasing number of sites with a schematic representation of the corresponding structures. The average degree of protonation θ is shown as a function of pH for generations $k = 0$, 1, and 2 with the corresponding number of sites being $N = 3(2^{k+1}) - 2$ ($N = 4$, 10, 22). On the scale of the graph, the $N \rightarrow \infty$ limit is approximately reached for $k = 6$ ($N = 190$); the curve presented corresponds to $k = 13$ ($N = 49150$).

each site on the outermost shell of the tree. In the next step one proceeds to the lower shell by evaluating all quantities of interest for all rooted subtrees. The process is continued until one reaches the lowest shell (i.e., the root of the original tree). The iteration process is readily programmed on a computer and results in a very efficient algorithm. One can easily obtain numerically exact results for trees with 10^5–10^8 sites. Already much smaller systems can be used as excellent approximations of the large system limit ($N \rightarrow \infty$).

3. Applications

In the following, we shall discuss titration curves which were calculated on the basis of Ising models for branched, treelike structures. First we shall investigate illustrative situations based on a idealized model where all ionizable sites have the equal microscopic pK values and interact by nearest neighbor pair interactions only. Later we shall address the titration curve of branched poly(ethylene imine) where different microscopic pK values of primary, secondary, and tertiary amines as well as various types of short range interactions are considered.

Model Systems. Focus first on the illustrative situation where all ionizable sites have the same microscopic value $p\hat{K} = 10$ and nearest neighbor pair interactions only, which will be characterized with the parameter $\epsilon = 2$. This model mimics poly(ethylene imine) in a semiquantitative fashion; more realistic models for these systems will be discussed further below. First we shall discuss *regular* structures; later *random* branched polyelectrolytes will be introduced.

Dendritic Polyelectrolytes. Consider first a dendrimer[16] which is also called a star(burst) polymer[17] or a Cayley tree.[13] The corresponding titration curves, which were calculated from of the exact recursion procedure described above, are shown in Figure 2 for

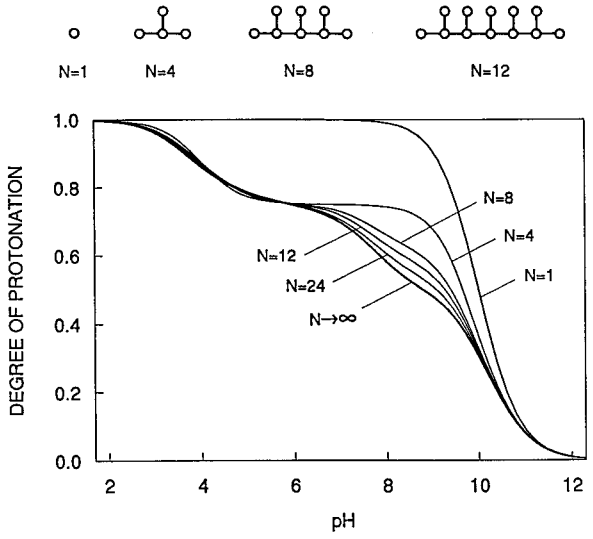

Figure 3. Calculated titration curves for comblike polyelectrolytes with increasing number of sites with a schematic representation of the corresponding structures. The average degree of protonation θ as a function of pH is given for an isolated site ($N = 1$) and for comblike polymers with linear chains of k triply coordinated sites, $k = 1$, 3, 5, 7, and 11, with corresponding total number of sites being $N = 2k + 2$ ($N = 4$, 8, 12, 16, 24). On the scale of the graph, the $N \rightarrow \infty$ limit is approximately reached for $k = 100$ ($N = 202$) and the curve presented corresponds to $k = 1001$ ($N = 2004$).

increasing denrimer size. One observes that the titration curves converge rather rapidly to the large system limit ($N \rightarrow \infty$). Runnels[14] asserts that for $\epsilon \gg 1$ no second-order phase transition (order–disorder transition) on such a Cayley tree is to be expected; this assertion is likely to be correct for any $\epsilon \geq 0$.

The first generation dendrimer is actually a simple model for tris(2-aminoethyl)amine. From the corresponding Ising model and eq 6, four macroscopic pK values can be calculated. These values are given in Table 1 (simple model). Around pH 10, all three singly coordinated terminal groups protonate (pH $\simeq p\hat{K}$); the splitting of the macroscopic pK values originates from entropy effects. The central triply coordinated group protonates at pH 4 since three pair interactions with a parameter $\epsilon = 2$ must be overcome (pH $\simeq p\hat{K} - 3\epsilon$). This splitting in the protonation of the terminal and central groups leads to the intermediate plateau at $\theta \simeq {}^3/_4$.

The titration curve of the infinitely large dendrimer ($N \rightarrow \infty$) can be understood in similar terms. At pH 10 only two-thirds of the sites protonate (pH $\simeq p\hat{K}$) while the remaining one-third of the sites protonate at much lower pH values (pH $\simeq p\hat{K} - 3\epsilon$). This protonation behavior originates from the "onion" shell structure of the dendrimer. At high pH the outermost sites in the first shell will protonate. Because of repulsive pair interactions, the second layer remains inert but the third layer can again protonate without involving any pair interactions. In the intermediate pH region every second shell of the dendrimer is protonated, which corresponds to two-thirds of all sites. Further protonation of the remaining shells happens around pH 4 as three pair interactions must be overcome.

Comblike Polyelectrolyte. With the dendrimer we have realized the most compact structure of the polymer; the least compact structure is the comblike polymer (a precise definition of the "compactness" is given in the Appendix). The titration curves of the comblike polyelectrolytes of different lengths are given in Figure 3. We note that the titration curves of the dendritic and

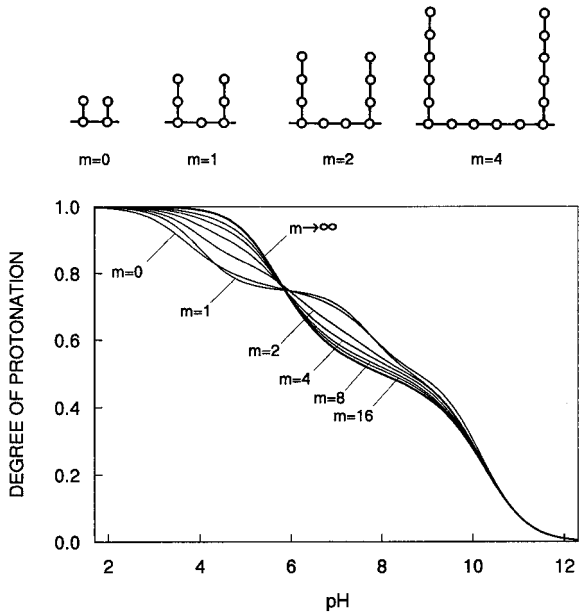

Figure 4. Calculated titration curves for comblike polyelectrolytes whose bonds have been replaced by linear chains of m doubly coordinated sites in the large system limit. Schematic representation of the corresponding structures, which contain singly, doubly and triply coordinated sites with a ratio of $1:2m:1$. For $m \to \infty$ one approaches the linear chain with pair interactions (cf. eq 12). Results for a comblike polyelectrolyte with $k = 1000$ are shown.

the comblike polylectrolyte are substantially different, eventhough both structures contain singly and triply coordinated groups only.

The titration curve of the infinitely large comblike polymer is again easily rationalized. Half of the sites on the comb can be occupied without invoking any nearest neighbor pair interactions (e.g., all singly coordinated groups). This process gives rise to the first protonation step around pH 10 ($\mathrm{pH} \simeq \mathrm{p}\hat{K}$). Protonation of an additional one-fourth of the sites can be achieved by invoking one pair interaction parameter which leads to the second step around pH 8 ($\mathrm{pH} \simeq \mathrm{p}\hat{K} - \epsilon$). This process results into an energetically stable state where all singly coordinated groups and every second triply coordinated groups is protonated. This state gives rise to the intermediate plateau at $^3/_4$. Additional protonation requires three pair interactions to be overcome which happens at pH 4 ($\mathrm{pH} \simeq \mathrm{p}\hat{K} - 3\epsilon$). As we shall see, this generic behavior will be relevant in other situations as well.

Regular Structures Involving Secondary Groups. Up to now, our examples did involve only sites with coordination numbers one (terminals) or three (branch points). Consider now the modifications introduced by the presence of doubly coordinated sites. The first example of such a structure will be generated from the comblike chain where we replace all bonds in the original comb with chains of m doubly coordinated sites. In the large system limit, the ratio of singly, doubly and triply coordinated sites is simply given by $1:2m:1$ (see Appendix). Clearly, for $m = 0$ the previously discussed case of a comblike polymer will be recovered, while as the chains connecting the branch points become very long ($m \to \infty$), the number of singly and triply coordinated sites becomes negligible, and the titration curve approaches the titration curve of a linear polyelectrolyte with nearest-neighbor interactions (cf. eq 12).

The transition between these two extremes is illustrated in Figure 4 where we display titration curves for comblike polymers in the large system limit where the original sites are jointed together with linear chains that consist of m doubly coordinated sites. As m increases, one recognizes a gradual transition from the titration curve of the original comblike polymer without doubly coordinated sites to the titration curve of a linear chain. We can observe that the titration curves for $m = 0$ and $m = 1$ are very similar. The reason for this behavior is interesting. Consider the situation for $m = 1$. Decreasing pH, we can first protonate half of the sites without invoking any pair interactions (e.g., by protonating all singly and half of the doubly coordinated sites). This process gives rise to the protonation step at pH 10 ($\mathrm{pH} \simeq \mathrm{p}\hat{K}$). At pH 8 we can protonate an additional one-fourth of the sites, since we have to overcome one pair interaction ($\mathrm{pH} \simeq \mathrm{p}\hat{K} - \epsilon$). After this process is completed, the system attains a low-energy state where all singly and doubly coordinated sites are protonated and all triply coordinated sites are deprotonated. The protonation of the remaining one-fourth of all sites, which are all triply coordinated, happens around pH 4 since three pair interactions must be overcome ($\mathrm{pH} \simeq \mathrm{p}\hat{K} - 3\epsilon$). Note that this is a very similar protonation scenario to the one that we have encountered for the original comblike polymer ($m = 0$). Consequently, the titration curves are rather similar in both cases ($m = 0$ and $m = 1$).

Remember that for polyelectrolytes without doubly coordinated groups ($m = 0$), the titration curves are substantially different for a dendrimer and for a comblike polymer; they depend quite sensitively on the compactness of the polymer. However, this dependence is almost completely lost as soon as at least one doubly coordinated groups is introduced between the sites of the original comblike polymer. For $m \geq 1$ the titration curves for a dendrimer and comblike polymer are virtually identical. Thus if doubly coordinated groups are present in the regular polyelectrolytes, the compactness of the polymer becomes an irrelevant variable. We shall see that a similar statement applies to randomly branched polyelectrolytes.

Randomly Branched Polyelectrolytes. As the final model example, let us discuss a branched polyelectrolyte with a random structure. Let us first use the (regular) dendrimer as the underlying structure and replace the bonds by chains of doubly coordinated sites. The random structure is generated by assuming that the length of these chains m is a random variable with a Poisson distribution with mean $\bar{m}$. As before, the ratio of singly, doubly, and triply coordinated sites is simply given by $1:2\bar{m}:1$ in the large system limit. Even though there will be many realizations of such random polymers, for a sufficiently large system, all individual realizations of the random polymer will lead to the same statistical average—a feature which is commonly referred to as the self-averaging property.[19]

In Figure 5 we show illustrative results in this large system limit. The randomness has washed out the structures observed in the regular systems and a rather generic titration curve is obtained. This titration curve has a rather weak dependence on the average chain length $\bar{m}$. Again, a scenario very similar to that discussed previously applies. Decreasing the pH, it is possible first to protonate half of the groups by avoiding all pair interactions. This processes happens around pH 10 and thereby all singly coordinated groups, but also some doubly or triply coordinated groups, are protonated. The remaining groups protonate continu-

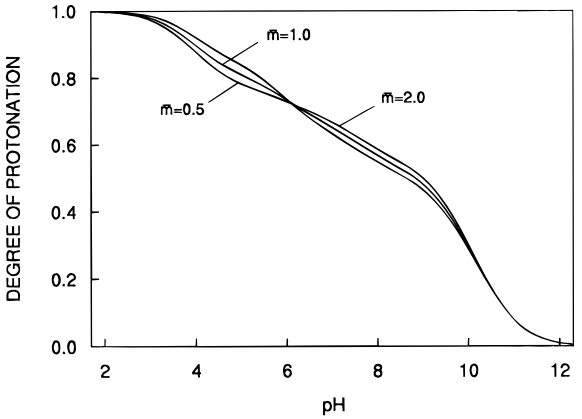

Figure 5. Calculated titration curves for random polyelectrolytes in the large system limit. The polymer is generated by replacing all bonds in a dendrimer by a chain of doubly coordinated sites of random lengths distributed according to a Poisson distribution with an average $\bar{m}$. For the values $\bar{m} =$ 0.5, 1.0, and 2.0 used here, the corresponding ratios of primary, secondary and tertiary groups are 1:1:1, 1:2:1, and 1:4:1 (1: $2\bar{m}$:1). Results for a dendrimer of generation $k = 10$ are shown with total number of sites $N \sim (1-4) \times 10^4$.

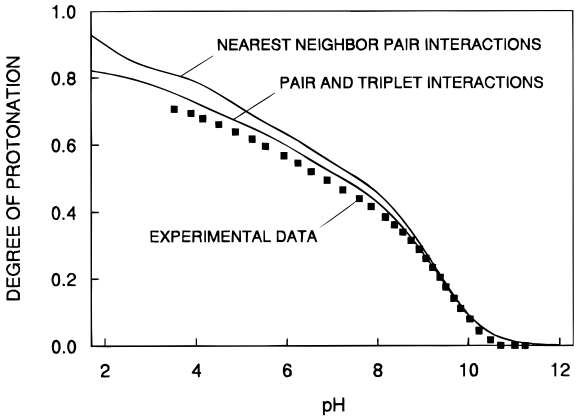

Figure 6. Experimental and calculated titration data of branched(polyethylene imine). Data points are experimental data in 0.5 mol/L NaCl by Balif et al.[5] Two kinds of calculations have been performed. The microscopic p$\hat{K}$ values of the primary, secondary and tertiary amines are 9.64, 8.59, and 7.50, respectively. The interaction parameters are $\epsilon = 1.85$ for nearest neighbor pairs, $\lambda = 0.42$ for nearest neighbor triplets, and $\epsilon' = 0.27$ for next nearest neighbor pairs across a tertiary groups. The more realistic model includes all these interactions; the simpler model neglects all but nearest neighbor pair interactions ($\lambda = \epsilon' = 0$). All parameters were determined independently; no parameter adjustment has been made. The structure is approximated by a random polymer as in Figure 5.

ously as pH decreases from 10 to 4. At first, the doubly coordinated groups protonate and finally the triply coordinated groups. The gradual protonation results from three overlaying protonation steps whereby, one, two, and three interactions must be overcome successively.

Further calculations show that as soon as the random polyelectrolyte contains a sufficient number of doubly coordinated sites, the compactness of the polymer has a very small influence on the titration curve. Approximately for $\bar{m} > 0.5$, the resulting titration curves are virtually identical for polyelectrolytes of either a compact structure (dendrimer) or a loose structure (treelike polymer). Since these two extreme cases of large and small compactness behave identically, all structures of intermediate compactness will behave in the same way. This observation particularly applies to polyelectrolytes where also the branching process is random in itself (see Appendix), However, the compactness of the polyelectrolyte becomes a relevant variable for small values of $\bar{m}$. In this situation, the titration curves are determined by a smooth crossover between both limiting cases (dendritic and comblike structures). This finding generalizes our observations for regular polyelectrolytes.

Branched Poly(ethylene imine). Various authors have investigated acid−base properties of branched poly(ethylene imine).[1−5] The titration curves resemble our results presented in Figure 5. About half of the sites are protonated in a rather narrow region around pH 10, while the remaining sites protonate continuously over a wide pH range. At pH 2 there is still a substantial fraction of the sites that remain to be protonated.

For a quantitative comparison, let us consider the experimental titration data of branched poly(ethylene imine) in 0.5 M NaCl by Balif et al.[5] Their data are reproduced here in Figure 6 with a minor modification for pH above 11. (Above this pH, the degree of protonation was reported to be slightly negative; these negative values were replaced by zero.) This polyelectrolyte has a molecular weight 10^5 to 3×10^6 ($N \sim 10^4$, practically the large system limit) and is suspected to have a ratio of primary, secondary, and tertiary groups of 1:2:1. This ratio corresponds to an average chain length of doubly coordinated sites $\bar{m} \simeq 1$. Viscosity measurements indicate a rather compact structure of the polyelectrolyte.[3]

Our interpretation is based on the available Ising model of linear poly(ethylene imine) and the corresponding oligomers.[6,10,11] Since we refer to the titration curve at an ionic strength of 0.5 M, a common parameter set at this ionic strength is rederived from available data for linear amines using the same methods as described previously.[11] We obtain for the microscopic p$\hat{K}$ values for the primary and secondary amine groups 9.64 and 8.59. Nearest neighbor pair and triplet interaction parameters have the values of $\epsilon = 1.85$ and $\lambda = 0.42$, respectively.

This information determines most of the parameters needed for the application of the Ising model to branched poly(ethylene imine). The remaining parameters were established as follows. For the tertiary amine group microscopic p$\hat{K}$ values in the range of 6−8 were suggested.[3,20] Here we employ a value of 7.50; a similar value was also proposed previously.[3] This value derives from a group additivity relationship.[20] The microscopic p$\hat{K}$ value of an amine group decreases by about one for every neighboring (deprotonated) amine attached to a β-carbon. The pK value of ethylamine of 10.66 at an ionic strength of 0.5 mol/L also fits into this scheme.[12] From pK values of tris(2-aminoethyl)amine given in Table 1 we estimate an interaction parameter $\epsilon' = 0.27$ for next nearest neighbor pair interactions which act across tertiary groups. The structure of branched poly(ethylene imine) was modeled by a dendrimer whose bonds were replaced by linear chains of secondary amine groups with random lengths distributed according to a Poisson distribution.

In Figure 6 we compare the experimental data with the prediction of the Ising model for such a branched polyelectrolyte. In the first, more realistic calculation we include all relevant interactions, namely nearest neighbor interactions for pairs and triplets as well as next nearest neighbor pair interactions. In the second, simplified calculation we only include the nearest

neighbor pair interactions. In the first case, the titration curve was obtained by performing a Monte Carlo simulation,[21] while in the second case the exact recursion relations were applied. (Naturally, we have verified that the Monte Carlo technique yields the same results in the latter case.)

In light of the fact that no parameter adjustment has been made, the agreement with the more realistic model is certainly satisfactory. Next nearest neighbor pair interactions and the nearest neighbor triplet interactions are essential to obtain quantitative agreement with experiment. The overall features of the titration curve are reflected semiquantitatively in the simpler model with nearest neighbor pair interactions only.

The remaining discrepancy could be due to the neglect of additional pair or triplet interactions, which we could not estimate from existing data on small molecules, due to the existence of closed loops or due to inaccuracies in the experimental data. By performing further calculations, we have verified that the compactness of the polymer, the length distribution of the secondary amine chains and its average, and the precise pK value of the tertiary amine group have little influence on the resulting titration curves.

4. Conclusion

The protonation behavior of branched polyelectrolytes can be rationalized by analyzing Ising models with short-range repulsive interactions. This situation is much more complex than for linear polyelectrolytes. The main difference in the protonation of the linear and branched polyelectrolytes is introduced by the triply coordinated sites in the branched structure. Given that the neighboring sites of a triply coordinated groups are already protonated, three pair interactions must be overcome, and this site will protonate at much lower pH values only. Even on the simplest nearest neighbor pair interaction level, various possible structures of branched polyelectrolytes necessarily lead to a wide spectrum of acid−base properties for this class of compounds and many types of titration curves follow. This richness is in marked contrast to the situation for linear polyelectrolytes. In the case of nearest neighbor pair interactions, only a single generic titration curve for a linear polyelectrolytes emerges.

For branched polyelectrolytes we have identified at least two fundamentally distinct protonation patterns: (i) The system protonates half of the sites at high pH. The remaining sites are protonated either in distinct steps or almost continuously over a wide pH range—triply coordinated sites protonate last. Examples of this protonation scheme include randomly branched polyelectrolytes with a substantial fraction of doubly coordinated sites or the comblike polyelectrolyte. The primary example for this protonation behavior is branched poly(ethylene imine). (ii) A rather different protonation pattern is revealed by dendrimers, which have a compact structure and consist of singly and triply coordinated sites only. The protonation of such compounds follows its "onion" shell structure whereby the odd shells, which comprise two-thirds of all ionizable sites, protonate at high pH while the even shells, which represent the remaining third, protonate at much lower pH. This protonation pattern is observed experimentally for poly(propylene imine) dendrimers.[18]

Acknowledgment. This paper is dedicated to Dieter Horn on the occasion of his 60th birthday. This work was supported by the ETH-Zürich and Swiss COST D5 program.

Appendix

Here we summarize the essential aspects of graph theory, which are needed for our developments (for details see refs 22 and 23). A *tree* is a connected graph without cycles (closed loops). The total number of bonds (edges) in a tree is $N - 1$ where N denotes the total number of sites (vertices). If we consider a maximum coordination number (valency) of three, the difference between the numbers of singly and triply coordinated sites is always two. These simple facts have a few consequences in the limit of large number of sites $N \rightarrow \infty$. The fraction of sites with coordination numbers one (terminals) and three (branch points) is the same. Denoting this fraction by x ($0 \leq x \leq {}^1/_2$) the fraction of doubly coordinated sites is given by $1 - 2x$. The average chain length of consecutive doubly coordinated sites is $\bar{m} = 1/(2x) - 1$. The average coordination number of all sites is two.

A *rooted tree* is a tree where one site is labeled (root vertex; see Figure 1). Sites lie on the same *shell* (or level) of a rooted tree if the root can be reached by passing the same number of sites. The *backbone* of a tree is obtained by deleting all dangling ends of the original tree.

The *skeleton* contains all information about the topology of a tree and is obtained by deleting all but the triply coordinated sites of the original tree and replacing the original connections with simple bonds. The skeleton of a comblike polymer is a linear chain, while for the dendrimer the skeleton is a (smaller) dendrimer. Thus the fraction of triply coordinated sites y on the skeleton ($0 \geq y \geq {}^1/_2$) represents an important characteristics of the topological structure of a given polymer, which we refer to as *compactness*. The most compact structure corresponds to a dendrimer ($y = {}^1/_2$) while the least compact structure is realized in the comblike polymer ($y = 0$).

A given tree can be defined in a unique fashion with a set of integers (molecular code). For our purposes we use a very simple code. If the sites of the associated skeleton are labeled with index i, the code consists of a vector c whose elements c_i are equal to the index of the site at the lower shell which is connected to site i. For the root r we choose $c_r = 0$. Sites can always be labeled such that $c_{i+1} \geq c_i$ and $c_1 = 0$ and $c_2 = 1$. For a dendrimer the vector c consist of a sequence of pairs of equal numbers (0,1,1,1,2,2,3,3,4,4,...) while for a comblike structure every number occurs only once (0,1,1,2,3,4,5,6,...). Each pair of equal numbers represents one triply coordinated site. A randomly branched polymer is generated by taking a random sequence of pairs and individual numbers. The original polymer is recovered by adding as many singly coordinates sites such that all sites of the skeleton have the coordination number three and then completing the appropriate number of doubly coordinated sites in between these sites.

References and Notes

(1) D. Horn in *Polymeric Amines and Ammonium Salts*; Goethals, E. J., Ed.; Pergamon Press: Oxford, England, 1980.
(2) von Zelewsky, A.; Barbosa, L.; Schläpfer, C. W. *Coord. Chem. Rev.* **1993**, *123*, 229.
(3) Bloys van Trenslong, C. J.; Staverman, A. J. *Recl. Trav. Chim. Pays-Bas* **1974**, *93*, 171. Bloys van Trenslong, C. J. *J. R. Neth. Chem. Soc.* **1974**, *97*, 13.

(4) Thiele, H.; Gronau, K. H. *Makromol. Chem.* **1989**, *59*, 207.
(5) Balif, J. B; Lerf, C.; Schläpfer, C. W. *Chimia* **1994**, *48*, 336.
(6) Smits, R. G.; Koper, G. J. M.; Mandel, M. *J. Phys. Chem.* **1993**, *97*, 5745.
(7) Marcus, R. A. *J. Phys. Chem.* **1954**, *58*, 621.
(8) Katchalsky, A.; Mazur, J.; Spitnik, P. *J. Polym. Sci.* **1957**, *23*, 513
(9) Reed, C. E.; Reed, W. F. *J. Chem. Phys.* **1992**, *96*, 1609.
(10) Borkovec, M.; Koper, G. J. M. *Ber. Bunsen-Ges. Phys. Chem.* **1996**, *100*, 764.
(11) Borkovec, M.; Koper, G. J. M. *J. Phys. Chem.* **1994**, *98*, 6038.
(12) Smith, R. M.; Martell, A. E. *Critical Stability Constants*; Plenum Press: New York, 1989; Vol. 6.
(13) Baxter, R. J. *Exactly Solved Models in Statistical Mechanics*; Academic Press: New York, 1982.
(14) Runnels, L. K. *J. Math. Phys.* **1967**, *8*, 2081.
(15) Müller-Hartmann, E.; Zittarz, J. *Phys. Rev. Lett.* **1974**, *33*, 893.
(16) Tomalia, D. A.; Baker, H.; Dewald, J.; Hall, M.; Kallos, G.; Martin, S.; Roeck, J.; Ryder, J.; Smith, P. *Polym. J.* **1985**, *17*, 117.
(17) de Gennes, P. G.; Hervet, H. *J. Phys. Lett.* **1983**, *44*, 351.
(18) van Duijvenbode, R.; Borkovec, M.; Koper, G. J. M. Manuscript in preparation.
(19) Mezard, M; Parisi, G; Virasoro, M. A. *Spin Glass Theory and Beyond*; World Scientific, Singapore, 1987; Section I.1.
(20) Perrin, D. D.; Dempsey B.; Serjeant, E. P. *pK_a Prediction for Organic Acids and Bases*; Chapman & Hall: London, 1981.
(21) Chandler D. *Introduction to Modern Statistical Mechanics*; Oxford University Press: New York, 1987.
(22) Trinajstić, N.; Nicolić, S.; Knop, J. V.; Müller, W. R.; Szymanski, K. *Computational Chemical Graph Theory*; Ellis Horwood: New York, 1991.
(23) Gordon, M.; Temple W. B. In *Chemical Applications of Graph Theory*; Balban A. T., Ed.; Academic Press: New York, 1976.

MA961312I